

This discussion paper is/has been under review for the journal Atmospheric Chemistry and Physics (ACP). Please refer to the corresponding final paper in ACP if available.

Temporal variation of elemental carbon in Guangzhou, China, in summer 2006

R. L. Verma¹, L. K. Sahu¹, Y. Kondo¹, N. Takegawa¹, S. Han¹, J. S. Jung²,
Y. J. Kim², S. Fan³, N. Sugimoto⁴, M. H. Shammaa¹, Y. H. Zhang⁵, and Y. Zhao⁶

¹Research Center for Advanced Science and Technology, University of Tokyo, Tokyo, Japan

²Advanced Environmental Monitoring Research Center, Department of Environmental Science and Engineering, Gwangju Institute of Science and Technology (GIST), Gwangju, Republic of Korea

³Institute of Environmental Meteorology, School of Environmental Science and Engineering, Sun Yat-sen University, Guangzhou, China

⁴Atmospheric Remote Sensing Section, National Institute for Environmental Studies, Tsukuba, Japan

⁵State Key Joint Laboratory of Environmental Simulation and Pollution Control, College of Environmental Science and Engineering, Peking University, Beijing, China

⁶Air Quality Research Center, University of California, Davis, USA

Received: 30 September 2009 – Accepted: 16 October 2009 – Published: 18 November 2009

Correspondence to: Y. Kondo (y.kondo@atmos.rcast.u-tokyo.ac.jp)

Published by Copernicus Publications on behalf of the European Geosciences Union.

Elemental carbon in Guangzhou

R. L. Verma et al.

Title Page

Abstract

Introduction

Conclusions

References

Tables

Figures

◀

▶

◀

▶

Back

Close

Full Screen / Esc

Printer-friendly Version

Interactive Discussion



Abstract

In situ measurements of the mass concentration of elemental carbon (EC) and mixing ratios of carbon monoxide (CO) and carbon dioxide (CO₂) were made at Guangzhou, an urban measurement site in the Pearl River Delta (PRD), China, in July 2006. The average±standard deviation (SD) concentrations of EC, CO, and CO₂ were 4.7±2.3 μgCm⁻³, 798±459 ppbv and 400±13 ppmv, respectively. The trends of these species were mainly controlled by synoptic-scale changes in meteorology during the campaign. Based on back trajectories, data are analyzed separately for two different air mass types representing northerly and southerly flows. Northerly air masses, constituting about 25% of the campaign, were mainly impacted by stagnant conditions, resulting in elevated levels of pollutants. On the other hand, southerly air masses measured during most of the campaign were mostly influenced by clean marine air. The diurnal patterns of EC, CO, and CO₂ exhibited peak concentrations during the morning and evening hours coinciding with rush-hour traffic. The diurnal variations of EC and ΔEC/ΔCO closely followed the traffic pattern of heavy-duty vehicles (HDV) in Guangzhou, similar to that observed in Beijing. The level of EC in this campaign was similar to values reported during previous studies at other sites surrounding Guangzhou. The average slopes of ΔEC/ΔCO, ΔEC/ΔCO₂, and ΔCO/ΔCO₂ were 0.0054 μgCm⁻³/ppbv, 0.15 μgCm⁻³/ppmv, and 46.4 ppbv/ppmv, respectively, agreeing reasonably well with their respective emission ratios derived from regional emission inventories.

1 Introduction

A major portion of the fine-mode aerosols in the urban atmosphere are carbonaceous aerosols. Carbonaceous aerosols are generally classified into organic carbon (OC) and elemental carbon (EC). EC is also referred to as black carbon (BC) and can ab-

Elemental carbon in Guangzhou

R. L. Verma et al.

Title Page

Abstract

Introduction

Conclusions

References

Tables

Figures

◀

▶

◀

▶

Back

Close

Full Screen / Esc

Printer-friendly Version

Interactive Discussion



**Elemental carbon in
Guangzhou**

R. L. Verma et al.

[Title Page](#)[Abstract](#)[Introduction](#)[Conclusions](#)[References](#)[Tables](#)[Figures](#)[◀](#)[▶](#)[◀](#)[▶](#)[Back](#)[Close](#)[Full Screen / Esc](#)[Printer-friendly Version](#)[Interactive Discussion](#)

sorb light, therefore acting as a positive radiative forcing agent in the troposphere and causing a negative radiative forcing at the earth surface (Ramanathan et al., 2008; Jacobson et al., 2000; Chuang et al., 2003; Kim et al., 2008). It has been estimated that the global mean clear-sky radiative forcing of BC is about $+0.4$ – 0.8 W/m² (IPCC, 2001). BC also affects cloud albedo and cloud formation (Conant et al., 2002; Nenes et al., 2002). Incomplete combustion of fossils fuels and biomass burning are the main sources of EC and CO. Quantitative information of their relative emissions can be used to characterize various emission sources (Hansen et al., 1989).

Emissions of various gaseous and particulate pollutants in Asia are increasing due to rapid industrialization and urban development (Streets et al., 2003). Elevated levels of the various aerosols and gaseous species in East Asian countries are of great concern because of their impacts on the atmospheric environment on regional and continental scales, for instance a reduction in precipitation of 10–20% and increasing tendency of floods and drought (Huang et al., 2007; Menon et al., 2002). In China, major economic expansion and industrialization are occurring in mega-city clusters like Beijing, Tianjin, Bohai, and the Pearl River Delta (PRD) (Shao et al., 2006). The PRD is a densely industrialized region where emissions from a large number of petrochemical, automobile, and electronics manufacturing units are significant. Guangzhou is the main commercial and industrial city in the PRD region, with an area of 7434.4 km² and population of over 10 million in the year 2006.

Previous studies of anthropogenic aerosols and gaseous pollutants at Guangzhou and the surrounding urban areas mostly focused on the relationships of OC and EC and their seasonal variations (Cao et al., 2003, 2004, 2007; Duan et al., 2007; Ho et al., 2006; Cheung et al., 2005). Some studies have also characterized aerosol chemical composition and optical properties (Andreae et al., 2008; Liu et al., 2008). However, none of the previous studies have reported the relationship of EC to other combustion tracers (e.g., CO, CO₂), particularly in light of their emission inventories from different sources. These relationships can be used to characterize sources and also to validate the existing emission inventories of these species. There is a need to study the diur-

nal variations of aerosols and gaseous species for their source attributions by making continuous time-resolved measurements.

For the first time, we report the temporal variations of hourly averaged EC, CO, and CO₂ in the PRD region in summer in light of transient meteorological conditions and diverse emission sources. We discuss the diurnal patterns of these species and slopes of $\Delta\text{EC}/\Delta\text{CO}$ in relation to traffic patterns. The estimated slopes of $\Delta\text{EC}/\Delta\text{CO}$, $\Delta\text{EC}/\Delta\text{CO}_2$, and $\Delta\text{CO}/\Delta\text{CO}_2$ are compared with respective emission ratios calculated from published emission inventories (Streets et al., 2003).

2 Measurement

2.1 Observation site

As a part of the Program of Regional Integrated Experiments of Air Quality over Pearl River Delta (PRIDE-PRD 2006) campaign, continuous measurements of EC, CO, and CO₂ concentrations were made at Guangzhou between 1 July and 31 July 2006. Figure 1a shows an emission map of EC from Guangzhou and the surrounding region (21.75–24.25° N and 112.25–114.75° E, 0.5°) for the year 2000 (Streets et al., 2003), while Fig. 1b shows the road network in the Guangzhou urban region. In Fig. 1a and b, a crossed circle represents the observation site, located on the 16th floor (~50 m above ground level (a.g.l.)) of the Guangdong Provincial Environmental Monitoring Center (GPEMC) building (23.13° N, 113.26° E). Guangzhou city is surrounded by a highway and major roads including an express highway, ring road, and Dongfeng road pass through the urban region. Dongfeng is the road closest to the observation site. Vehicular activity on the Dongfeng road is discussed in Sect. 3.

2.2 Experimental

Measurements of EC mass concentration in the fine-mode (PM_{2.5}) were made using a semi-continuous carbon aerosol analyzer (RT 3015, Sunset Laboratory Inc., US) with

24632

Elemental carbon in Guangzhou

R. L. Verma et al.

Title Page

Abstract

Introduction

Conclusions

References

Tables

Figures

◀

▶

◀

▶

Back

Close

Full Screen / Esc

Printer-friendly Version

Interactive Discussion



**Elemental carbon in
Guangzhou**

R. L. Verma et al.

[Title Page](#)[Abstract](#)[Introduction](#)[Conclusions](#)[References](#)[Tables](#)[Figures](#)[◀](#)[▶](#)[◀](#)[▶](#)[Back](#)[Close](#)[Full Screen / Esc](#)[Printer-friendly Version](#)[Interactive Discussion](#)

one-hour time resolution. The analysis of elemental and organic carbon (EC-OC) was based on the National Institute for Occupational Safety and Health (NIOSH) thermal-optical transmittance (TOT) protocol for pyrolysis correction (Birch and Cary, 1996; Jeong et al., 2004; Kim et al., 2006). Ambient air samples were drawn through an inlet line fitted with a cyclone with a $2.5\ \mu\text{m}$ particle diameter ($\text{PM}_{2.5}$) sharp cut-off size at a flow rate of 8 LPM. Then the samples were passed through a carbon-impregnated filter (CIF) multi-channel parallel-plate denuder to remove volatile organic vapors (VOCs). Samples were collected on quartz filter paper for 44 min and then heated in four stages at increasing temperatures under a helium atmosphere to quantify the carbonaceous aerosols. As the OC vaporized during temperature ramping, it was oxidized to CO_2 in the oxidizing oven. EC was oxidized to CO_2 when the temperature was stepped up to 850°C in the oven in an oxygen environment. The instrument was calibrated by auto-injection of CH_4 (5% in He) as an internal standard. The detection limit of the instrument was estimated to be $0.4\ \mu\text{gCm}^{-3}$, determined as three times the standard deviation (σ) of a filtered air measurement (dynamic blank). The measurement uncertainty of the instrument was estimated to be 5%. The detection limit and measurement uncertainty were similar to those reported by Polidori et al. (2006), Jeong et al. (2004), Kim et al. (2006), and Jung et al. (2009) for the EC-OC analyzer.

The mixing ratio of CO was measured using a non-dispersive infrared (NDIR) absorption gas analyzer (Model 48, Thermo Environmental Instruments (TEI), US) with an integration time of one minute. CO_2 concentration was measured using an NDIR-based instrument (Model LI 7000, LI-Cor, Inc., United States) with an integration time of 10 s (Kondo et al., 2006; Takegawa et al., 2006). A common inlet line (Teflon tube of internal diameter (ID) $\sim 6\text{mm}$ and length $\sim 10\text{m}$) was used for both analyzers from the rooftop. Because of high relative humidity levels at the measurement site in summer, air samples were passed through two sets of Nafion dryers (Perma-Pure Inc., USA) before analysis to reduce the interference of water vapor. On-site calibrations of CO and CO_2 were performed using standard mixtures with 5 ppmv of CO in air and 358 ppmv and 639 ppmv of CO_2 in air. The accuracy and precision of the CO measurements

were 1.4% and 4 ppbv (at CO=400ppbv in 1 min), while for CO₂ these were 0.2% and 0.3 ppmv (at CO₂=400ppmv in 10 s), respectively. Further details of these analyzers were reported by Takegawa et al. (2009).

Meteorological data were obtained from the nearest meteorological station (ZDQ-13), manufactured and operated by Sun Yet-san University, China. The accuracies of meteorological parameters like wind speed, wind direction, ambient temperature, ambient pressure, and rainfall were about $\pm 0.3\text{ms}^{-1}$, $\pm 5^\circ$ (at wind speed 0.5ms^{-1}), 0.2°C , 0.2hPa , and 0.4mmh^{-1} , respectively. The Mixed Layer Height (MLH) or the depth of the Planetary Boundary Layer (PBL) was estimated from the vertical profiles of aerosol extinction coefficient at a wavelength of 1064 nm from a Light Detection and Ranging (LIDAR) system operated by the National Institute for Environmental Studies (NIES), Japan. The MLH is defined as the height where the gradient of the attenuated backscattering coefficient (ATBC) at 1064 nm is a minimum. Details of the LIDAR measurements during the PRD campaign were discussed by Sugimoto et al. (2009).

3 Emissions of EC, CO, and CO₂

Figure 1a shows the spatial distribution of emissions of EC. Although not shown emissions of CO and CO₂ exhibit similar distributions in Guangzhou and the surrounding urban region (Streets et al., 2003). The observation site is located within the grid ($0.5^\circ \times 0.5^\circ$) of highest emissions of EC, while other major emission grids are distributed in the southeast (SE) corridors. These major EC emissions are mainly from the urban areas of Guangzhou, Foshan, Shenzhen, Zhongshan, and Jiangmen, in decreasing order. Apart from the emission sources in Guangzhou, the impact of anthropogenic activities in Foshan city could be significant, as it is the urban region closest to the measurement site. Foshan is the third largest manufacturing base in the PRD region, after Shenzhen and Guangzhou. Emissions from the sources located along the north-west (NW) and northeast (NE) sectors are less, compared to the contributions from the southern regions. Table 1 illustrates the emissions of EC, CO, and CO₂ from domestic

Elemental carbon in Guangzhou

R. L. Verma et al.

Title Page

Abstract

Introduction

Conclusions

References

Tables

Figures

◀

▶

◀

▶

Back

Close

Full Screen / Esc

Printer-friendly Version

Interactive Discussion



**Elemental carbon in
Guangzhou**

R. L. Verma et al.

Title Page

Abstract

Introduction

Conclusions

References

Tables

Figures

◀

▶

◀

▶

Back

Close

Full Screen / Esc

Printer-friendly Version

Interactive Discussion



and non-domestic sectors for the year 2000 (Streets et al., 2003). The domestic sector is further sub-categorized as biofuels and fossil fuels, collectively contributing about 30% of EC and 10–15% each of CO and CO₂ to the total emissions. The non-domestic sector includes emissions from industry, power generation, transport, ships, etc. and contributes about 70% of EC and 85–90% each of CO and CO₂. Among these sources emissions from industry and transport mainly contribute to the non-domestic sector (Streets et al. 2003, unpublished data). However, these inventories contain large uncertainties, viz., 484% for EC, 156% for CO, and 16% for CO₂ for China (Streets et al., 2003).

Traffic exhaust is an important source of anthropogenic emissions in the Guangzhou urban regions (Zhou et al., 2007; Shao, 2001). Figure 2 illustrates the hourly averaged diurnal variations of traffic volume comprising heavy-duty (HDV), medium-duty (MDV), and light-duty vehicles (LDV) on the Dongfeng Middle Road recorded during 18–24 July 1999 and 12–18 October 1999 (Xie et al., 2003). These traffic data were recorded 7 years before the present study; however, we assume that the diurnal pattern remains nearly unchanged. The total traffic volume is lowest during early morning hours, increases after about 07:00 LT, peaks between 07:00–11:00 LT, and then decreases gradually until midnight. However, HDVs show a different pattern remaining nearly stable during the day and late evening hours (Fig. 2). There was no traffic regulation in Guangzhou for entry restrictions for heavy-duty vehicles in city area before July 2007 (<http://www.chinacourt.org/flwk/show1.php?file-id=118290>) as it is in Beijing to avoid the traffic jam (Han et al., 2009). It is important to note that the emission factor of EC in HDV exhaust is significantly higher than LDV and MDV (Westerdahl et al., 2009 and references therein).

4 Temporal variations of EC, CO, CO₂, and meteorological conditions

Figure 3 shows temporal variations of hourly averaged EC, CO, CO₂, and some meteorological parameters. The average \pm SD of wind speed, temperature, relative humidity,

**Elemental carbon in
Guangzhou**

R. L. Verma et al.

Title Page

Abstract

Introduction

Conclusions

References

Tables

Figures

◀

▶

◀

▶

Back

Close

Full Screen / Esc

Printer-friendly Version

Interactive Discussion



and pressure were $2.6 \pm 1 \text{ ms}^{-1}$, $31 \pm 3^\circ\text{C}$, $76 \pm 14\%$, and $1003 \pm 5 \text{ hPa}$, respectively, during the campaign. Meteorological conditions were fairly stable, with steady wind flow ($\sim 3 \text{ ms}^{-1}$) from the South China Sea during 2–11 July. The concentration of EC remained constant at $\sim 4 \mu\text{gCm}^{-3}$ for this period, except for two episodes of elevated levels in the early morning of 3 July and evening of 7 July. Observations during 12–13 July were impacted by rather weak northerly flow ($< 2 \text{ ms}^{-1}$). These stagnant weather conditions could have favored the accumulation of recently emitted pollutants, resulting in higher EC and CO of $\sim 12.5 \mu\text{gCm}^{-3}$ and $\sim 1700 \text{ ppbv}$, respectively. A typhoon (named Billis) originating over the southern oceanic region hit the PRD on 15 July and continued until 17 July. Significant amounts of these species were likely scavenged by the rain associated with the strong wind flow during the typhoon circulation (Fig. 3). Relatively lower concentrations of pollutants were observed until 18 July due to dilution caused by the mixing of cleaner air. No significant changes in the concentrations of EC or CO were observed during 19–22 July. Later, during 23–26 July, observations were influenced by stagnant weather, and consequently EC and CO reached levels of $15.0 \mu\text{gCm}^{-3}$ and 2500 ppbv , respectively, on some occasions. Another typhoon event, named Kaemi, arrived over the PRD with strong winds and rain during 27–28 July. The long-term trend of CO_2 mixing ratio was similar to that of EC and CO. To avoid any bias, measurements conducted during the episodes of rainfall have been excluded from the statistical and correlation analyses.

Generally, the concentrations of EC, CO, and CO_2 appear to have been influenced by changes in meteorological conditions. To investigate the impact of long-range transport of the air masses, 3 – day isobaric back trajectories were calculated using the Hybrid Single Particle Lagrangian Integrated Trajectory (HYSPPLIT-4) model (Draxler and Rolph, 2003) (see Fig. 4). Each trajectory starts at 00:00 LT (local time) and 50 m a.g.l. at the measurement site. Based on the analyses of the entire period of observations, the air masses at the Guangzhou site have been classified into two main categories depending on the direction of transport, from northerly (red line in Fig. 4) and southerly (blue line in Fig. 4) directions. The southerly air masses originated over the South

**Elemental carbon in
Guangzhou**

R. L. Verma et al.

[Title Page](#)[Abstract](#)[Introduction](#)[Conclusions](#)[References](#)[Tables](#)[Figures](#)[◀](#)[▶](#)[◀](#)[▶](#)[Back](#)[Close](#)[Full Screen / Esc](#)[Printer-friendly Version](#)[Interactive Discussion](#)

China Sea (SCS) and prevailed during 1–11 July, 16–22 July, and 27–31 July, influencing ~75% of the entire campaign. Air masses categorized as northerly air (~25% of the measurements) arrived from the NW and NE directions and influenced the observations during 12–14 July and 23–26 July, which were also the periods of elevated levels of pollutants.

Data measured in both northerly and southerly air masses are further classified into two categories, day (08:00–18:00 LT) and night (20:00–06:00 LT). The daytime measurements represent observations of well-mixed air due to both higher boundary layer depth and wind speed. Statistics of EC, CO, CO₂, and wind speed measured in the different categories of air masses are presented in Table 2. The average ±SD (day+night) mass concentration of EC and mixing ratio of CO in the northerly air masses were 6.3±2.4 μgCm⁻³ and 1059±589 ppbv, while these were 4.3±1.9 μgCm⁻³ and 693±327 ppbv in the southerly air masses, respectively. The levels of EC and CO were about 30% higher in the northerly air masses than those in the southerly air masses. Based on all measured data the average concentrations of EC, CO, and CO₂ were 4.7±2.3 μgCm⁻³, 798±459 ppbv, and 400±13 ppmv, respectively.

During northerly flow, the meteorological conditions favored stagnation, causing higher levels of pollutants in ambient air. In contrast, southerly air masses were generally dominated by cleaner marine air from the South China Sea (Liu et al., 2008; Lai et al., 2007; Yeung et al., 2006). We have estimated the background concentrations, illustrated in Table 3. The background concentration is defined as the 1.25 percentile of the dataset (Kondo et al., 2006). The background concentrations of both EC and CO in the northerly air masses were higher by about a factor of two than those estimated for southerly air masses.

5 Diurnal variations

Diurnal plots of the hourly average ±SD of EC, CO, CO₂, wind speed, and MLH for both northerly and southerly air masses are shown in Fig. 5. The diurnal variations in

**Elemental carbon in
Guangzhou**

R. L. Verma et al.

Title Page

Abstract

Introduction

Conclusions

References

Tables

Figures

◀

▶

◀

▶

Back

Close

Full Screen / Esc

Printer-friendly Version

Interactive Discussion



these species are particularly strong during northerly flow. The concentrations of EC, CO, and CO₂ start increasing from the early morning hours (05:00–06:00 LT), reaching their peaks at around 07:00–09:00 LT. As the day advances, the levels of these species decrease gradually during the afternoon (13:00–15:00 LT) due to higher vertical mixing caused by a simultaneous increase in wind speed and MLH. In the evening hours, concentrations of EC, CO, and CO₂ exhibit increasing trends before their peaks at around 19:00–21:00 LT. Their peak concentrations coincide with the rush hours and therefore can be attributed mainly to traffic emissions. Similar features have been reported from measurements in other urban regions (Glasius et al., 2006; Park et al., 2005; Latha et al., 2004; Baumgardner et al., 2007; Dutkiewicz et al., 2009). Variations of EC concentration closely follow the traffic pattern of HDVs, suggesting their major influence (Fig. 6). As we have discussed the emission factor of EC from HDVs is higher than other vehicles. Thus peaks in EC can be attributed mainly to the emissions from HDVs, as the combustion of diesel fuel in these vehicles is an important source of EC (Bond et al., 2004). Emissions from other sources mainly from industrial and domestic activities can also contribute to the observed levels of these species (see Table 1).

As can be seen in Fig. 5, EC and CO exhibit elevated concentrations and strong diurnal variations in northerly air compared to that observed during southerly flow. These characteristic differences in the features of diurnal variability could be attributed mainly to the variations in the regional-scale transport and meteorology. The elevated levels of pollutants in northerly air can be due to both local emissions and transport of polluted continental air from northern China. On the other hand, southerly air brings cleaner marine air, which can dilute the locally emitted pollutants, resulting in the observed lower concentrations of trace species. During the afternoon hours the MLH and wind speed reached maximum values; therefore, levels of these species were observed to be the lowest. The diurnal features in the two different air mass types are also supported by different meteorological conditions; for example, in the early morning hours (06:00–09:00 LT) the MLH for northerly air was shallower by ~500m than that during southerly flow. In other words, observed lower levels of EC, CO, and CO₂ in the southerly air flow

could be due to the availability of more space for dilution. The significant differences in MLH for the two different air mass types coincide with the rush hours, and as a result the amplitudes of peaks in EC, CO, and CO₂ were much larger in northerly air. We observed that day-to-night ratios of all trace species were higher in the southerly air compared to that during northerly flow. The transport from strong daytime emission sources situated in the south of Guangzhou could have counterbalanced the dilution due to increased MLH (http://www.idsgroup.com/profile/pdf/industry_series/LFIndustrial2.pdf).

6 Dependence of EC on wind and MLH

Apart from the local time dependence of the emissions, variations in meteorological parameters can influence the concentrations of pollutants; however, their contributions cannot be separated in a strict sense. Considering the significant variability in meteorology during daytime the data observed between 09:00 to 21:00 LT has been used to study the dependencies of EC on wind and MLH (Fig. 7). In the lower wind speed regime, for example from 0.5 to 1.0 ms⁻¹, the concentration of EC decreases sharply from about 9 μgCm⁻³ to 6 μgCm⁻³ in southerly air masses, while in the higher wind speed regime, say 1.0–5.0 ms⁻¹, EC decreases gradually from 6 μgCm⁻³ to 3 μgCm⁻³. Similarly EC also decreases with wind speed in northerly air, but its level was always higher than that of southerly. Similar relationships between EC and wind speed have been observed at other urban locations, including Tokyo (Kondo et al., 2006) and Beijing (Han et al., 2009). However, the concentration of EC does not show any systematic dependence on MLH for either air mass types. This relationship with MLH also explains that the levels of EC could have been influenced by strong daytime emissions. The presence of stable aerosol layers above the boundary layer could have also inhibited the dilution of EC due to increasing MLH (Sugimoto et al., 2009).

Elemental carbon in Guangzhou

R. L. Verma et al.

Title Page

Abstract

Introduction

Conclusions

References

Tables

Figures

◀

▶

◀

▶

Back

Close

Full Screen / Esc

Printer-friendly Version

Interactive Discussion



7 Relationship between EC, CO, and CO₂

The roles of major factors impacting the diurnal variation of EC can be further investigated by estimating emission ratios of EC to other combustion products like CO and CO₂, as reported by Kondo et al. (2006) and Han et al. (2009). A diurnal plot of the slope of $\Delta EC/\Delta CO$, calculated from a bi-variable linear fit regression method, is shown in Fig. 8. Hourly data were used for southerly air masses, while a 3-hourly interval was used for northerly air masses due to limited data. Data points with poor correlations ($r^2 < 0.35$) are not shown in Fig. 8. In the southerly air masses, the slope of $\Delta EC/\Delta CO$ increases from about 06:00 LT before a peak value ($\sim 0.011 \mu\text{gCm}^{-3}/\text{ppbv}$) at about 09:00 LT; later it decreases sharply and remains at about $0.005 \mu\text{gCm}^{-3}/\text{ppbv}$ during the afternoon. In the evening hours, $\Delta EC/\Delta CO$ again increases and peaks ($\sim 0.0093 \mu\text{gCm}^{-3}/\text{ppbv}$) at 19:00 LT. The diurnal variation of $\Delta EC/\Delta CO$ closely follows the patterns of HDV and MDV traffic (see Fig. 2). Therefore the observed slope of $\Delta EC/\Delta CO$ represents the emission ratios from HDVs and MDVs particularly during the peak hours.

In addition to the characterization of major sources of EC, CO, and CO₂ emissions, the slopes of $\Delta EC/\Delta CO$, $\Delta EC/\Delta CO_2$, and $\Delta CO/\Delta CO_2$ can be useful in investigating the transport of EC from source regions. For example, $\Delta CO/\Delta CO_2$ ratios have been used to identify the origin of air masses (Takegawa et al., 2004). Estimates of the transport efficiency of EC from source region to the boundary layer and from the boundary layer to the free troposphere have been based on EC/CO correlation slopes and emission ratios calculated from emission inventories (Sahu et al., 2008). Figure 9 shows scatter plots of the pairs EC-CO, EC-CO₂, and CO-CO₂ using all data. Table 4 illustrates details of linear fit regression slopes of $\Delta EC/\Delta CO$, $\Delta EC/\Delta CO_2$, and $\Delta CO/\Delta CO_2$. The slopes of $\Delta EC/\Delta CO$ and $\Delta EC/\Delta CO_2$ of daytime data are lower than those at nighttime in both types of air masses, whereas $\Delta CO/\Delta CO_2$ shows the opposite pattern (Table 4). Reliable $\Delta EC/\Delta CO$ slopes are useful for assessing long-range transport of EC with reference to CO. The linear fit re-

Elemental carbon in Guangzhou

R. L. Verma et al.

[Title Page](#)[Abstract](#)[Introduction](#)[Conclusions](#)[References](#)[Tables](#)[Figures](#)[◀](#)[▶](#)[◀](#)[▶](#)[Back](#)[Close](#)[Full Screen / Esc](#)[Printer-friendly Version](#)[Interactive Discussion](#)

gression slopes of $\Delta EC/\Delta CO$, $\Delta EC/\Delta CO_2$, and $\Delta CO/\Delta CO_2$ over the whole dataset are $0.0054 \mu\text{gCm}^{-3}/\text{ppbv}$, $0.15 \mu\text{gCm}^{-3}/\text{ppmv}$, and $46.4 \text{ ppbv}/\text{ppmv}$, respectively.

8 Comparisons

8.1 Guangzhou and Beijing

5 Guangzhou and Beijing are two major urban regions of China where vehicular emissions can be important source of ambient EC. In this study, we have compared the diurnal relations of EC with traffic of heavy-duty vehicles in both cities (see Fig. 10). Similar to our observations, the diurnal variation of EC follows the traffic of heavy-duty diesel trucks (HDDTs) in Beijing (Han et al., 2009). In Beijing, the concentration of EC
10 shows a diurnal cycle opposite to that observed in Guangzhou, as it was observed to be higher (lower) during the night (day). Similarly the traffic volume also shows the opposite diurnal patterns in these cities. Kondo et al. (2006) also report a close relationship of ambient EC with traffic in Tokyo. The present and previous studies in urban regions suggest that the concentrations of ambient EC are mainly controlled by the
15 emissions from heavy duty-vehicles.

8.2 Previous observations

For the first time we report hourly time-resolved measurements of EC at Guangzhou. Here we compare mean EC concentration observed in the present study with previous measurements conducted at different sites in Guangzhou during the summer
20 (Fig. 11). The EC concentration of $4.7 \mu\text{gCm}^{-3}$ in this study agrees well with a range of $4.6\text{--}5.7 \mu\text{gCm}^{-3}$ measured at Zhongshan University (8 km from GPMEC) (Cao et al., 2003), Liwan (5 km), and Wushan (19 km) (Duan et al., 2007). Slightly higher EC concentrations of 7.9 and $6.5 \mu\text{gCm}^{-3}$ were observed at Huangpu ($\sim 17\text{km}$) and Longgui ($\sim 28\text{km}$), respectively (Cao et al., 2004). Huangpu is a heavily industrialized (e.g.,

Elemental carbon in Guangzhou

R. L. Verma et al.

Title Page

Abstract

Introduction

Conclusions

References

Tables

Figures

◀

▶

◀

▶

Back

Close

Full Screen / Esc

Printer-friendly Version

Interactive Discussion



**Elemental carbon in
Guangzhou**

R. L. Verma et al.

Title Page

Abstract

Introduction

Conclusions

References

Tables

Figures

◀

▶

◀

▶

Back

Close

Full Screen / Esc

Printer-friendly Version

Interactive Discussion



chemical, metallurgical) district of Guangzhou where emissions from power plants and vehicular exhaust are also important (Tan et al., 2006; Bi et al., 2003). Although Longgui is considered a background site, the cause of elevated EC is unknown (Cao et al., 2004). EC measured in summer is lower than the average values of $7.1 \mu\text{gCm}^{-3}$ in spring (Andreae et al., 2008) and $14.5 \mu\text{gCm}^{-3}$ in winter (Cao et al., 2007). A comparison of observed EC and $\Delta\text{EC}/\Delta\text{CO}$ with that reported for other major urban regions of Asia is shown in Table 5. The EC mass concentration and slopes of $\Delta\text{EC}/\Delta\text{CO}$ in Guangzhou are comparable to those observed in Beijing (China), Gwanju and Seoul (South Korea), Hyderabad (India), and Karachi (Pakistan). These results are expected as traffic emissions are known to be the major source of EC and CO in these urban regions. However, these EC concentrations are significantly higher than that measured in Tokyo. The values of $\Delta\text{EC}/\Delta\text{CO}_2$ and $\Delta\text{CO}/\Delta\text{CO}_2$ at Guangzhou (Table 4) agree reasonably with $0.12\text{--}0.19 \mu\text{gCm}^{-3}/\text{ppmv}$ and $30.2\text{--}43.9 \text{ppbv}/\text{ppmv}$, respectively, in Beijing, and the slopes of $\Delta\text{CO}/\Delta\text{CO}_2$ in Guangzhou and Beijing are significantly higher than that of $11.2 \text{ppbv}/\text{ppmv}$ in Tokyo. This comparison suggests that measurements in Tokyo are influenced by emissions from efficient fuel combustion processes.

8.3 Correlation slopes and emission ratios

To understand the importance of major emission sources impacting the levels of EC, CO, and CO_2 in the Guangzhou urban region, the slopes of $\Delta\text{EC}/\Delta\text{CO}$, $\Delta\text{EC}/\Delta\text{CO}_2$, and $\Delta\text{CO}/\Delta\text{CO}_2$ are compared with the emission ratios derived from emission factors reported for different sources (Table 6) and emission inventories (Table 7). In Table 6 ranges of emission ratios of EC-CO, EC- CO_2 , and CO- CO_2 are presented for different sectors. The observed slopes of $\Delta\text{EC}/\Delta\text{CO}$ ($0.0054 \mu\text{gCm}^{-3}/\text{ppbv}$), $\Delta\text{EC}/\Delta\text{CO}_2$ ($0.15 \mu\text{gCm}^{-3}/\text{ppmv}$), and $\Delta\text{CO}/\Delta\text{CO}_2$ ($46.4 \text{ppbv}/\text{ppmv}$) in this study at Guangzhou are within the range of emissions ratios estimated for diesel fuel and gasoline combustion in the transport sector. However, contributions from combustion processes in other sectors can also influence the observed slopes of these species.

**Elemental carbon in
Guangzhou**

R. L. Verma et al.

[Title Page](#)[Abstract](#)[Introduction](#)[Conclusions](#)[References](#)[Tables](#)[Figures](#)[I◀](#)[▶I](#)[◀](#)[▶](#)[Back](#)[Close](#)[Full Screen / Esc](#)[Printer-friendly Version](#)[Interactive Discussion](#)

Comparison of observed slopes of $\Delta EC/\Delta CO$, $\Delta EC/\Delta CO_2$, and $\Delta CO/\Delta CO_2$ with their emission ratios derived from the inventories can be useful to validate the inventory data. However, this study has its limitations because ambient air may not be homogeneously mixed as various emissions sources are collocated. The emission ratios of EC/CO, EC/CO₂, and CO/CO₂ derived for the urban regions of Guangzhou (21.75–24.25° N, 112.25–114.75° E), Beijing, and Tokyo using Streets et al. (2003) inventory data for the year 2000 are shown in Table 7. These emission ratios were derived by summing the emissions from the domestic and non-domestic sectors (Streets et al., 2003). For Guangzhou, the observed slopes of $\Delta EC/\Delta CO$, $\Delta EC/\Delta CO_2$, and $\Delta CO/\Delta CO_2$ agree reasonably with the respective emission ratios (Tables 4 and 7). Therefore, the observed slopes validate the emissions inventories of EC, CO, and CO₂, to some extent. However, this statement may not be entirely conclusive considering the limited measurements for this study and uncertainties in the inventories. In support of our discussion, the estimated EC/CO emissions ratio of $0.0049 \mu\text{gCm}^{-3}/\text{ppbv}$ from the transport sector (Streets et al., 2003; unpublished dataset) agrees well with the observed slope of $0.0054 \mu\text{gCm}^{-3}/\text{ppbv}$. Emission ratios of the Guangzhou urban region also agree well with those estimated for Beijing but not with those of Tokyo (Table 7).

9 Conclusions

As part of the PRIDE-PRD 2006 campaign, measurements of EC mass concentration, mixing ratios of CO and CO₂, and meteorological parameters were conducted at an urban site in Guangzhou, China during July 2006. Guangzhou is the main industrial and commercial city of the PRD region, where emissions due to road transport, industrial, and domestic activities are the major sources of pollutants. The traffic volume was highest during morning hours; however, unlike other categories of vehicles, traffic of heavy-duty vehicles was remained high during the daytime. The average concentrations of EC, CO, and CO₂ were $4.7 \mu\text{gCm}^{-3}$, 798 ppbv and 400 ppmv, respectively, during the campaign. Trends in EC, CO, and CO₂ concentrations were influenced by local

**Elemental carbon in
Guangzhou**

R. L. Verma et al.

Title Page

Abstract

Introduction

Conclusions

References

Tables

Figures

◀

▶

◀

▶

Back

Close

Full Screen / Esc

Printer-friendly Version

Interactive Discussion



meteorology and episodes of typhoons. The trajectory analysis suggests the influence of cleaner marine air from the southern direction during most of the campaign, while stagnant conditions prevailed during northerly flow leading to observed higher background levels of EC and CO by a factor of about two than those during southerly flow.

5 The diurnal patterns of EC, CO, and CO₂ exhibited primary peaks during the morning and secondary peaks in the evening hours coinciding with rush-hour traffic. In addition to the traffic emissions the variability in meteorological parameters played a key role in the observed diurnal variations of these species. The diurnal patterns of EC and $\Delta\text{EC}/\Delta\text{CO}$ closely followed the patterns of HDV and MDV traffic. Similar to studies reported for Beijing and Tokyo cities, EC showed a close relationship with the heavy-duty vehicle traffic in Guangzhou. The EC measured in the present study agrees reasonably well with previous measurements reported for summer at nearby sites in Guangzhou. Similar values of EC and slopes of $\Delta\text{EC}/\Delta\text{CO}$ are comparable to those reported at several urban regions in Asia. Observed slopes of $\Delta\text{EC}/\Delta\text{CO}$ ($0.0054 \mu\text{gCm}^{-3}/\text{ppbv}$), $\Delta\text{EC}/\Delta\text{CO}_2$ ($0.15 \mu\text{gCm}^{-3}/\text{ppmv}$) and $\Delta\text{CO}/\Delta\text{CO}_2$ ($46.4 \text{ppbv}/\text{ppmv}$) agree reasonably with respective emission ratios, validating the inventories to some extent.

Acknowledgement. This work was supported by the Ministry of Education, Culture, Sports, Science and Technology (MEXT), the global environment research fund of the Japanese Ministry of Environment (B-083), and the Japanese Science and Technology Agency (JST). This work was conducted as a part of the Mega-Cities: Asia Task under the framework of the International Global Atmospheric Chemistry (IGAC) project.

References

- Andreae, M. O. and Metlet, P.: Emission of trace gases and aerosols from biomass burning, *Global Biochem. Cy.*, 15(4), 955–966, 2001.
- 25 Andreae, M. O., Schmid, O., Yang, H., Chanda, D., Yu, J. Z., Zeng, L. M., and Zhang, Y. H.: Optical properties and chemical composition of the atmospheric aerosol in urban Guangzhou, China, *Atmos. Environ.*, 42, 6335–6350, 2008.

**Elemental carbon in
Guangzhou**

R. L. Verma et al.

Title Page

Abstract

Introduction

Conclusions

References

Tables

Figures

◀

▶

◀

▶

Back

Close

Full Screen / Esc

Printer-friendly Version

Interactive Discussion



Baumgardner, D., Kok, G. L., and Raga, G. B.: On the diurnal variability of particle properties related to light absorbing carbon in Mexico City, *Atmos. Chem. Phys.*, 7, 2517–2526, 2007, <http://www.atmos-chem-phys.net/7/2517/2007/>.

Bi, X., Sheng, G., Peng, P., Chen, Y., Zhang, Z., and Fu, J.: Distribution of particulate- and vapor-phase n-alkanes and polycyclic aromatic hydrocarbons in urban atmosphere of Guangzhou, China, *Atmos. Environ.*, 37, 289–298, 2003.

Birch, M. E. and Cary, R. A.: Elemental carbon-based method for monitoring occupational exposures to particulate diesel exhaust, *Aerosol Sci. Tech.*, 25, 221–241, 1996.

Bond, T. C., Streets, D. G., Yarber, K. F., Nelson, S. M., Woo, J. H., and Klimont, Z.: A technology-based global inventory of black and organic carbon emissions from combustion, *J. Geophys. Res.* 109, D14203, doi:10.1029/2003JD003697, 2004.

Boucher, O. and Reddy, M. S.: Climate trade-off between black carbon and carbon dioxide emissions, *Energy Policy*, 36, 193–200, doi:10.1016/j.enpol.2007.08.039, 2008.

Cao, J. J., Lee, S. C., Ho, K. F., Zhang, X. Y., Zou, S. C., Fung, K., Chow, J. C., and Watson, J. G.: Characteristics of carbonaceous aerosol in Pearl River Delta Region, China during 2001 winter period, *Atmos. Environ.*, 37, 1451–1460, 2003.

Cao, J. J., Lee, S. C., Ho, K. F., Zou, S. C., Fung, K., Lib, Y., Watson, J. G., and Chow, J. C.: Spatial and seasonal variations of atmospheric organic carbon and elemental carbon in Pearl River Delta Region, China, *Atmos. Environ.*, 38, 4447–4456, 2004.

Cao, J. J., Lee, S. C., Chow, J. C., Watson, J. G., Ho, K. F., Zhang, R. J., Jin, Z. D., Shen, Z. X., Chen, G. C., Kang, Y. M., Zou, S. C., Zhang, L. Z., Qi, S. H., Dai, M. H., Cheng, Y., and Hu, K.: Spatial and seasonal distributions of carbonaceous aerosols over China, *J. Geophys. Res.*, 112, D22S11, doi:10.1029/2006JD008205, 2007.

Cao, G., Zhang, X., Gong, S., and Zheng, F.: Investigation on emission factors of particulate matter and gaseous pollutants from crop residue burning, *J. Environ. Sci.*, 20, 50–55, 2007.

Cheung, H. C., Wang, T., Baumann, K., and Guo, H.: Influence of regional pollution outflow on the concentrations of fine particulate matter and visibility in the coastal area of southern China, *Atmos. Environ.*, 39, 6463–6474, 2005.

Chuang, P. Y., Duvall, R. M., Bae, M. S., Jefferson, A., Schauer, J. J., Yang, H., Yu, J. Z., and Kim, J.: Observations of elemental carbon and absorption during ACE-Asia and implications for aerosol radiative properties and climate forcing, *J. Geophys. Res.*, 108(D23), 8634, doi:10.1029/2002JD003254, 2003.

Conant, W. C., Nenes, A., and Seinfeld, J. H.: Black carbon radiative heating effects on cloud

**Elemental carbon in
Guangzhou**

R. L. Verma et al.

Title Page

Abstract

Introduction

Conclusions

References

Tables

Figures

◀

▶

◀

▶

Back

Close

Full Screen / Esc

Printer-friendly Version

Interactive Discussion



- microphysics and implications for aerosol indirect forcing, 1, Extended Köhler theory, *J. Geophys. Res.*, 107(D21), 4604, doi:10.1029/2002JD002094, 2002.
- Dhammapala, R., Claiborn, C., Simpson, C., and Jimenez, J.: Emission factors from wheat and Kentucky bluegrass stubble burning: Comparison of field and simulated burn experiments, *Atmos. Environ.*, 41, 1512–1520, doi:10.1016/j.atmosenv.2006.10.008, 2007.
- Dickerson, R. R., Andreae, M. O., Campos, T., Mayol-Bracero, O. L., Neusuess, C., and Streets, D. G.: Analysis of black carbon and carbon monoxide observed over the Indian Ocean: Implications for emissions and photochemistry, *J. Geophys. Res.*, 107(D19) 8017, doi:10.1029/2001JD000501, 2002.
- Draxler, R. R. and Rolph, G. D.: HYSPLIT (HYbrid Single-Particle Lagrangian Integrated Trajectory) Model access via NOAA ARL READY, NOAA Air Resources Laboratory, Silver Spring, MD, website (<http://www.arl.noaa.gov/ready/hysplit4.html>), 2003.
- Duan, J., Tan, J., Cheng, D., Bi, X., Deng, W., Sheng, G., Fu, J., and Wong, M. H.: Sources and characteristics of carbonaceous aerosol in two largest cities in Pearl River Delta Region, China, *Atmos. Environ.*, 41, 2895–2903, 2007.
- Dutkiewicz, V. A., Alvi, S., Ghauri, B. M., Choudhary, M. I., and Husain, L.: Black carbon aerosols in urban air in South Asia, *Atmos. Environ.*, 43, 1737–1744, doi:10.1016/j.atmosenv.2008.12.043, 2009.
- Glasiusa, M., Ketzel, M., Wahlin, P., Jensen, B., Mønster, J., Berkowicz, R., and Palmgren, F.: Impact of wood combustion on particle levels in a residential area in Denmark, *Atmos. Environ.*, 40, 7115–7124, 2006.
- Han, S., Kondo, Y., Takegawa, N., Miyazaki, Y., Oshima, N., Hu, M., Lin, P., Deng, Z., Zhao, Y., and Sugimoto, N.: Temporal variation of elemental carbon in Beijing, *J. Geophys. Res.*, doi:10.1029/2009JD012027, in press, 2009.
- Hansen, A. D. A., Convey, T. J., Steele, L. P., Bodhaine, B. A., Thoning, K. W., Tans, P., and Novakov, T.: Correlations among combustion effluent species at Barrow, Alaska: Aerosol black carbon, carbon dioxide, and methane, *J. Atmos. Chem.*, 9, 283–299, 1989.
- Ho, K. F., Lee, S. C., Cao, J. J., Li, Y. S., Chow, J. C., Watson, J. G., and Fung, K.: Variability of organic and elemental carbon, water soluble organic carbon, and isotopes in Hong Kong, *Atmos. Chem. Phys.*, 6, 4569–4576, 2006, <http://www.atmos-chem-phys.net/6/4569/2006/>.
- Huang, Y., Chameides, W. L., and Dickinson, R. E.: Direct and indirect effects of anthropogenic aerosols on regional precipitation over east Asia, *J. Geophys. Res.*, 112, D03212,

doi:10.1029/2006JD007114, 2007.

Intergovernmental Panel on Climate Change (IPCC): http://www.grida.no/publications/other/ipcc_tar/?src=/climate/ipcc_tar/, 2001.

Jacobson, M. Z.: A physically-based treatment of elemental carbon optics: Implications for global direct forcing of aerosols, *Geophys. Res. Lett.*, 27(2), 217–220, 2000.

Jeong, C. H., Hopke, P. K., Kim, E., and Lee, D. W.: The comparison between thermal-optical transmittance elemental carbon and Aethalometer black carbon measured at multiple monitoring sites, *Atmos. Environ.*, 38, 5193–5204, 2004.

Jung, J. S., Lee, H., Kim, Y. J., Liu, X., Zhang, Y., Gu, J., and Fan, S.: Aerosol chemistry and the effect of aerosol water on visibility impairment and radiative forcing in Guangzhou during the 2006 Pearl River Delta campaign (PRIDE-PRD2006), *J. Environ. Manage.*, 90, 3231–3244, 2009.

Kim, D. and Ramanathan, V.: Solar radiation budget and radiative forcing due to aerosols and clouds, *J. Geophys. Res.*, 113, D02203, doi:10.1029/2007JD008434, 2008.

Kim, Y. J., Kim, M. J., Lee, K. H., and Park, S. S.: Investigation of carbon pollution episodes using semi-continuous instrument in Incheon, Korea, *Atmos. Environ.*, 40, 4064–4075, 2006.

Kondo, Y., Komazaki, Y., Miyazaki, Y., Moteki, N., Takegawa, N., Kodama, D., Deguchi, S., Nogami, M., Fukuda, M., Miyakawa, T., Morino, Y., Koike, M., Sakurai, H., and Ehara, K.: Temporal variations of elemental carbon in Tokyo, *J. Geophys. Res.*, 111, D12205, doi:10.1029/2005JD006257, 2006.

Lai, S. C., Zou, S. C., Cao, J. J., Lee, S. C., and Ho, K. F.: Characterizing ionic species in PM_{2.5} and PM₁₀ in four Pearl River Delta cities, South China, *J. Environ. Sci.*, 19, 939–947, ISSN:1001-0742, CN 11-2629/X, 2007.

Latha, K. M. and Badarinath, K. V. S.: Correlation between black carbon aerosols, carbon monoxide and tropospheric ozone over a tropical urban site, *Atmos. Res.*, 71, 265–274, 2004.

Liu, X., Cheng, Y., Zhang, Y., Jung, J., Sugimoto, N., Chang, S. Y., Kim, Y. J., Fan, S., and Zeng, L.: Influences of relative humidity and particles chemical composition on aerosol scattering properties during the 2006 PRD campaign, *Atmos. Environ.*, 42, 1525–1536, 2008.

Menon S., Hansen, J., Nazarenko, L., and Luo, Y.: Climate Effects of Black Carbon Aerosols in China and India, *Science*, 297, 2250–2253 doi:10.1126/science.1075159, 2002.

Nenes, A., Conant, W. C., and Seinfeld, J. H.: Black carbon radiative heating effects on cloud microphysics and implications for the aerosol indirect effect, 2, *Cloud microphysics*, *J. Geo-*

Elemental carbon in Guangzhou

R. L. Verma et al.

Title Page

Abstract

Introduction

Conclusions

References

Tables

Figures

◀

▶

◀

▶

Back

Close

Full Screen / Esc

Printer-friendly Version

Interactive Discussion



**Elemental carbon in
Guangzhou**

R. L. Verma et al.

Title Page

Abstract

Introduction

Conclusions

References

Tables

Figures

◀

▶

◀

▶

Back

Close

Full Screen / Esc

Printer-friendly Version

Interactive Discussion



phys. Res., 107(D21), 4605, doi:10.1029/2002JD002101, 2002.

Park, S. S., Bae, M. S., Schauer, J. J., Ryu, S. S., Kim, Y. J., Cho, S. Y., and Kim, S. J.: Evaluation of the TMO and TOT methods for OC and EC measurement and their characteristics in PM_{2.5} at an urban site of Korea during ACE-Asia, *Atmos. Environ.*, 39, 5101–5112, 2005.

5 Park, S. S., Kim, Y. J., and Kang, C. H.: Polycyclic aromatic hydrocarbons in bulk PM_{2.5} and size-segregated aerosol particle samples measured in an urban environment, *Environ. Monit. Assess.*, 128, 231–240, doi:10.1007/s10661-006-9308-4, 2007.

Polidori, A., Turpin, B. J., Lim, H. J., Cabada, J. C., Subramanian, R., Pandis, S. N., Robinson, A. L.: Local and regional secondary organic aerosol: Insights from a year of semi-

10 continuous carbon measurements at Pittsburg, *Aerosol Sci. Tech.*, 40, 861–872, 2006.

Ramanathan, V. and Carmichael, G.: Global and regional climate changes due to black carbon, *Nat. Geosci.*, 1, 221–227, doi:10.1038/ngeo156, 2008.

Sahu, L. K., Kondo, Y., Miyazaki, Y., Kuwata, M., Koike, M., Takegawa, N., Tanimoto, H., Matsueda, H., Yoon, S. C., and Kim, Y. J.: Anthropogenic aerosols observed in Asian continental outflow at Jeju Island, Korea, in spring 2005, *J. Geophys. Res.*, 114, D03301, doi:10.1029/2008JD010306, 2009.

Sanchez-Ccoyllo, O. R., Ynoue, R. Y., Martins, L. D., Astolfo, R., Miranda, R. M., Freitas, E. D., Borges, A. S., Fornaro, A., Freitas, H., Moreira, A., and Andrade, M. F.: Vehicular particulate matter emissions in road tunnels in Sao Paulo, Brazil, *Environ. Monit. Assess.*, 149, 241–

20 249, doi:10.1007/s10661-008-0198-5, 2009.

Shao, M., Tang, X., Zhang, Y., and Li, W.: City clusters in China: Air and surface water pollution, *Front. Ecol. Environ.*, 4(7), 353–361, 2006.

Shao, M. and Zhang, Y.: Current Air quality problem and control strategies for Vehicular emissions in China, website (<http://www.walshcarlines.com/china/china.airquality.minshao.pdf>), 2001.

25 Streets, D. G., Bond, T. C., Carmichael, G. R., Fernandes, S. D., Fu, Q., He, D., Klimont, Z., Nelson, S. M., Tsai, N. Y., Wang, M. Q., Woo, J. H., and Yarber, K. F.: An inventory of gaseous and primary aerosol emissions in Asia in the year 2000, *J. Geophys. Res.*, 108(D21), 8809, doi:10.1029/2002JD003093, 2003.

30 Sugimoto, N., Nishizawa, T., Liu, X., Matsui, I., Shimizu, A., Zhang, Y., Kim, Y. J., Li, R., and Liu, J.: Continuous observations of aerosol profiles with a two-wavelength Mie-cattering lidar in Guangzhou in PRD2006, *J. Appl. Meteorol. Clim.*, 48, 1822–1830, doi:10.1175/2009JAMC2089.1, 2009.

**Elemental carbon in
Guangzhou**

R. L. Verma et al.

[Title Page](#)[Abstract](#)[Introduction](#)[Conclusions](#)[References](#)[Tables](#)[Figures](#)[◀](#)[▶](#)[◀](#)[▶](#)[Back](#)[Close](#)[Full Screen / Esc](#)[Printer-friendly Version](#)[Interactive Discussion](#)

- Takegawa, N., Kondo, Y., Koike, M., Chen, G., Machida, T., Watai, T., Blake, D. R., Streets, D. G., Woo, J. H., Carmichael, G. R., Kita, K., Miyazaki, Y., Shirai, T., Liley, J. B., and Ogawa, T.: Removal of NO_x and NO_y in Asian outflow plumes: Aircraft measurements over the western Pacific in January 2002, *J. Geophys. Res.*, 109, D23S04, doi:10.1029/2004JD004866, 2004.
- 5 Takegawa, N., Miyakawa, T., Kondo, Y., Jimenez, J. L., Zhang, Q., Worsnop, D. R., and Fukuda, M.: Seasonal and diurnal variations of submicron organic aerosol in Tokyo observed using the aerodyne aerosol mass spectrometer, *J. Geophys. Res.*, 111, D11206, doi:10.1029/2005JD006515, 2006.
- Takegawa, N., Miyakawa, T., Kuwata, M., Kondo, Y., Zhao, Y., Han, S., Kita, K., Miyazaki, Y.,
10 Deng, Z., Xiao, R., Hu, M., Van Pinxteren, D., Herrmann, H., Hofzumahaus, A., Holland, F., Wahner, A., Blake, D. R., Sugimoto, N., and Zhu, T.: Variability of submicron aerosol observed at a rural site in Beijing in the summer of 2006, *J. Geophys. Res.*, 114, D00G05, doi:10.1029/2008JD010857, 2009.
- Tan, J. H., Bi, X. H., Duan, J. C., Rahn, K. A., Sheng, G. Y., and Fu, J. M.: Seasonal variation
15 of particulate polycyclic aromatic hydrocarbons associated with PM_{10} in Guangzhou, China, *Atmos. Res.*, 80, 250–262, 2006.
- Westerdahl, D., Wang, X., Pan, X., and Zhang, K. M.: Characterization of on-road vehicle emission factors and microenvironmental air quality in Beijing, China, *Atmos. Environ.*, 42, 697–705, 2009.
- 20 Xie, S., Zhang, Y., Qi, L., and Tang, X.: Spatial distribution of traffic-related pollutant concentrations in street canyons, *Atmos. Environ.*, 37, 3213–3224, 2003.
- Yeung, M. C., Lee, S. C., Lun, B. H., and Tanner, P. A.: Summer rain events in south-east Asia: Spatial and temporal variations, *Atmos. Res.*, 86, 241–248, 2007.
- Zhou, K., Ye, Y. H., Liu, Q., Liu, A. J., and Peng, H. L.: Evaluation of ambient air quality in
25 Guangzhou, China, *J. Environ. Sci.*, 19, 432–437, 2007.

Elemental carbon in Guangzhou

R. L. Verma et al.

Table 1. Relative contributions (in %) of EC, CO, and CO₂ emissions from different sources in Guangzhou urban area (21.75–24.25 °N and 112.25 – 114.75° E) for the year 2000 (Streets et al., 2003)^a.

	Domestic sector ^a		Industry	Power	Non-domestic sector ^b		Total
	Fossils fuel	Biofuel			Transportation		
EC	10 (2.0)	21 (4.1)	38 (7.8)	2 (0.5)	28 (5.8)	100 (20.4)	
CO	3 (101.7)	10 (337.8)	47 (1624.1)	2 (66.1)	39 (1347.4)	100 (3477.2)	
CO ₂	5 (8140.0)	6 (10 020.6)	32 (50 481.0)	39 (61 507.4)	17 (26 540.1)	100 (156 689.1)	

() Emissions of each species (in Ggyr⁻¹)

^a Streets et al. (2003) (published data)

^b Streets et al. (2003) (unpublished inventory dataset)

Title Page

Abstract

Introduction

Conclusions

References

Tables

Figures

◀

▶

◀

▶

Back

Close

Full Screen / Esc

Printer-friendly Version

Interactive Discussion



Elemental carbon in
Guangzhou

R. L. Verma et al.

Table 2. Statistics of EC, CO, CO₂, and wind speed, observed in different categories at Guangzhou.

		EC (μgCm^{-3})				CO (ppbv)				CO ₂ (ppmv)				Wind speed (ms^{-1})			
		Min.	Max.	Mean \pm SD	Median	Min.	Max.	Mean \pm SD	Median	Min.	Max.	Mean \pm SD	Median	Min.	Max.	Mean \pm SD	Median
North	Day	2.7	12.9	5.8 \pm 2.4	5.2	429	2282	1025 \pm 441	909	383	452	402 \pm 14	400	0.9	4.8	2.9 \pm 0.9	2.8
	Night	3.9	18.7	6.8 \pm 2.5	6.3	443	3107	1092 \pm 737	803	383	446	410 \pm 14	408	0.4	5.7	2.4 \pm 0.9	2.4
South	Day	1.2	9.7	4.1 \pm 1.4	3.8	315	2729	734 \pm 315	688	373	436	396 \pm 11	395	0.6	5.1	2.7 \pm 0.9	2.5
	Night	1.1	17.0	4.4 \pm 2.4	3.8	263	1991	652 \pm 338	556	380	452	397 \pm 10	395	0.2	4.0	2.2 \pm 0.9	2.3
All data		1.1	18.7	4.7 \pm 2.3	4.2	202	3162	798 \pm 459	685	373	453	400 \pm 13	398	0.2	5.7	2.6 \pm 1.0	2.5

Title Page

Abstract

Introduction

Conclusions

References

Tables

Figures

I◀

▶I

◀

▶

Back

Close

Full Screen / Esc

Printer-friendly Version

Interactive Discussion



**Elemental carbon in
Guangzhou**

R. L. Verma et al.

Table 3. The background concentrations (1.25 percentiles) of EC, CO, and CO₂.

		EC (μgCm^{-3})	CO (ppbv)	CO ₂ (ppmv)
North	Day	2.79	430	383
	Night	3.88	448	386
South	Day	2.33	333	376
	Night	1.57	295	383
All data		1.92	322	379

Title Page

Abstract

Introduction

Conclusions

References

Tables

Figures

I◀

▶I

◀

▶

Back

Close

Full Screen / Esc

Printer-friendly Version

Interactive Discussion



Elemental carbon in Guangzhou

R. L. Verma et al.

Table 4. Observed EC-CO, EC-CO₂, and CO-CO₂ linear regressions slopes (± 1 SD) .

		$\Delta EC/\Delta CO$ ($\mu\text{gCm}^{-3}/\text{ppbv}$)		$\Delta EC/\Delta CO_2$ ($\mu\text{gCm}^{-3}/\text{ppmv}$)		$\Delta CO/\Delta CO_2$ (ppbv/ppmv)	
		r^2	r^2	r^2	r^2	r^2	r^2
North	Day	0.0045 \pm 0.0004	0.68	0.13 \pm 0.1	0.62	49.4 \pm 3.1	0.60
	Night	0.0069 \pm 0.0008	0.58	NA	–	NA	–
South	Day	0.0051 \pm 0.0005	0.59	0.12 \pm 0.1	0.55	57.4 \pm 1.9	0.46
	Night	0.0070 \pm 0.0004	0.75	0.21 \pm 0.1	0.76	34.9 \pm 1.5	0.67
All data	Day	0.0045 \pm 0.0005	0.51	0.13 \pm 0.1	0.57	53.2 \pm 1.9	0.50
	Night	0.0067 \pm 0.0004	0.72	0.16 \pm 0.1	0.55	NA	–
All data		0.0054 \pm 0.0002	0.61	0.15 \pm 0.1	0.58	46.4 \pm 1.5	0.45

NA: not available

[Title Page](#)
[Abstract](#)
[Introduction](#)
[Conclusions](#)
[References](#)
[Tables](#)
[Figures](#)
[Back](#)
[Close](#)
[Full Screen / Esc](#)
[Printer-friendly Version](#)
[Interactive Discussion](#)


Elemental carbon in
Guangzhou

R. L. Verma et al.

Table 5. The concentrations of EC aerosol and linear fit regression slopes measured in major urban regions of Asia.

Place and measurement period	EC (μgCm^{-3})	$\Delta\text{EC}/\Delta\text{CO}$ ($\mu\text{gCm}^{-3}/\text{ppbv}$)	Method of EC analysis	References
Guangzhou, China (Jul 2006)	4.7	0.0054	TOT	Present study
Guangzhou, China (Oct–Nov 2004)	7.1	0.0079	TOT	Andreae et al. (2008)
Beijing, China (2005–2006)	6.9	0.0035–0.0058	TOT	Han et al. (2009)
Tokyo, Japan (2003–2005)	1.9	0.0057	TOT	Kondo et al. (2006)
Gwanju, South Korea (Mar–May 2001)	5.7	0.0060	TOT	Park et al. (2005)
Seoul, South Korea (1998–1999)	4.5	0.0022	TMO	Park et al. (2007)
Hyderabad, India (Jan 2004)	1.5–11.2	0.0073	L. Abs.	Latha et al. (2004)
Karachi, Pakistan (2006–2007)	5.9	NA	L. Abs.	Dutkiewicz et al. (2009)

(): r^2

NA: not available

TOT: thermal-optical-transmittance

TMO: Thermal manganese dioxide oxidation

L. Abs.: Light absorption

Title Page

Abstract

Introduction

Conclusions

References

Tables

Figures

I◀

▶I

◀

▶

Back

Close

Full Screen / Esc

Printer-friendly Version

Interactive Discussion



Elemental carbon in
Guangzhou

R. L. Verma et al.

Table 6. EC/CO ($\mu\text{gCm}^{-3}/\text{ppbv}$), EC/CO₂ ($\mu\text{gCm}^{-3}/\text{ppmv}$), and CO/CO₂ (ppbv/ppmv) emissions ratios derived from emission factors (grams of pollutant evolved per kilogram of fuel burned).

	Transport		Industry	Domestic		Biomass burning
	Diesel ^{d,e,g,h}	Gasoline ^{d,h}	Coal ^d	Coal ^{d,f}	biofuels ^{c,d}	(crop residue) ^{a,b,c}
EC/CO	0.0013–0.055	0.0031–0.0115	0.0017–0.0182	0.0019–0.0572	0.0087–0.0266	0.0056–0.016
EC/CO ₂	0.15	0.06–0.11	0.04–0.74	0.11–3.56	0.69–1.75	0.53–1.10
CO/CO ₂	8.6–65.2	33.5	23.5–40.4	53.3–62.2	52.9–98.5	45.7–123.6

^a Dhammapala et al. (2007)

^b Cao et al. (2008)

^c Andreae and Merlet (2001)

^d Streets et al. (2003)

^e Dickerson et al. (2002)

^f Boucher et al. (2008)

^g Sanchez et al. (2009)

^h Westerdahl et al. (2009)

Title Page

Abstract

Introduction

Conclusions

References

Tables

Figures

I◀

▶I

◀

▶

Back

Close

Full Screen / Esc

Printer-friendly Version

Interactive Discussion



**Elemental carbon in
Guangzhou**

R. L. Verma et al.

[Title Page](#)[Abstract](#)[Introduction](#)[Conclusions](#)[References](#)[Tables](#)[Figures](#)[I◀](#)[▶I](#)[◀](#)[▶](#)[Back](#)[Close](#)[Full Screen / Esc](#)[Printer-friendly Version](#)[Interactive Discussion](#)

Table 7. Emissions ratios derived from the inventory of Streets et al. (2003) for major urban regions in Asia.

	EC/CO ($\mu\text{gCm}^{-3}/\text{ppbv}$)	EC/CO ₂ ($\mu\text{gCm}^{-3}/\text{ppmv}$)	CO/CO ₂ (ppbv/ppmv)
Guangzhou	0.0067	0.23	35.0
Beijing	0.0050	0.24	47.6
Tokyo	0.0093	0.082	8.8

Elemental carbon in
Guangzhou

R. L. Verma et al.

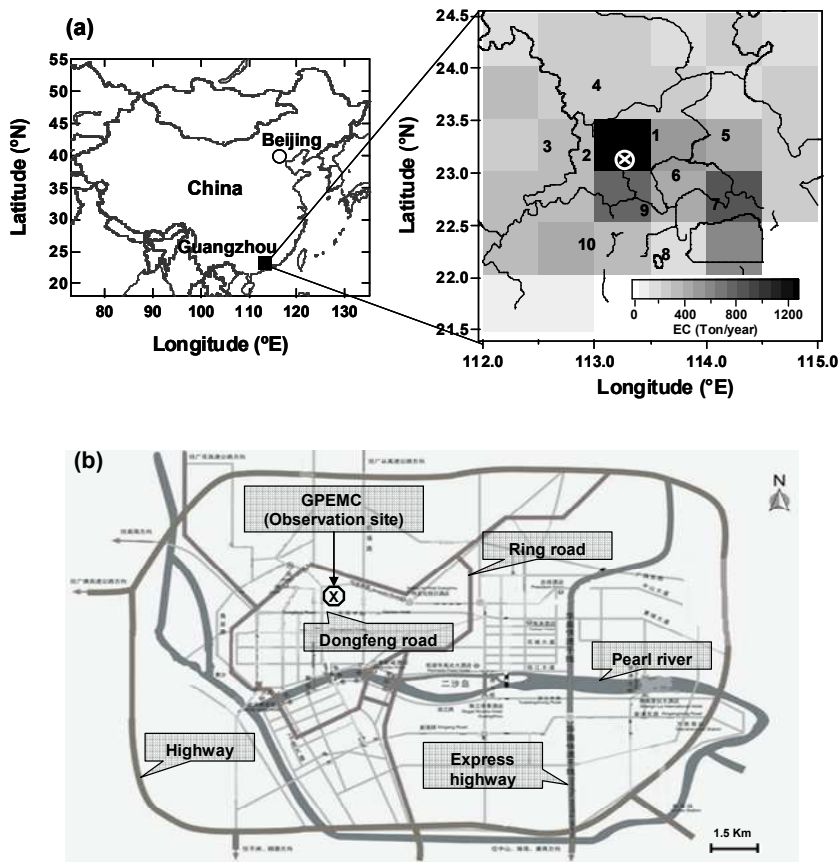


Fig. 1. (a) Spatial distribution of EC emissions (tons/yr) in Guangzhou and surrounding areas ($21.75\text{--}24.25^\circ\text{N}$ and $112.25\text{--}114.75^\circ\text{E}$). Numeric labels are for: 1. Guangzhou, 2. Foshan, 3. Zhouqing, 4. Qianguan, 5. Huizhou, 6. Dongguan, 7. Shenzhen, 8. Zhuhai, 9. Zhongshan, 10. Jiangmen. White circled cross represents observation site. (b) Road network surrounding the observation site in Guangzhou.

[Title Page](#)[Abstract](#)[Introduction](#)[Conclusions](#)[References](#)[Tables](#)[Figures](#)[I◀](#)[▶I](#)[◀](#)[▶](#)[Back](#)[Close](#)[Full Screen / Esc](#)[Printer-friendly Version](#)[Interactive Discussion](#)

Elemental carbon in
Guangzhou

R. L. Verma et al.

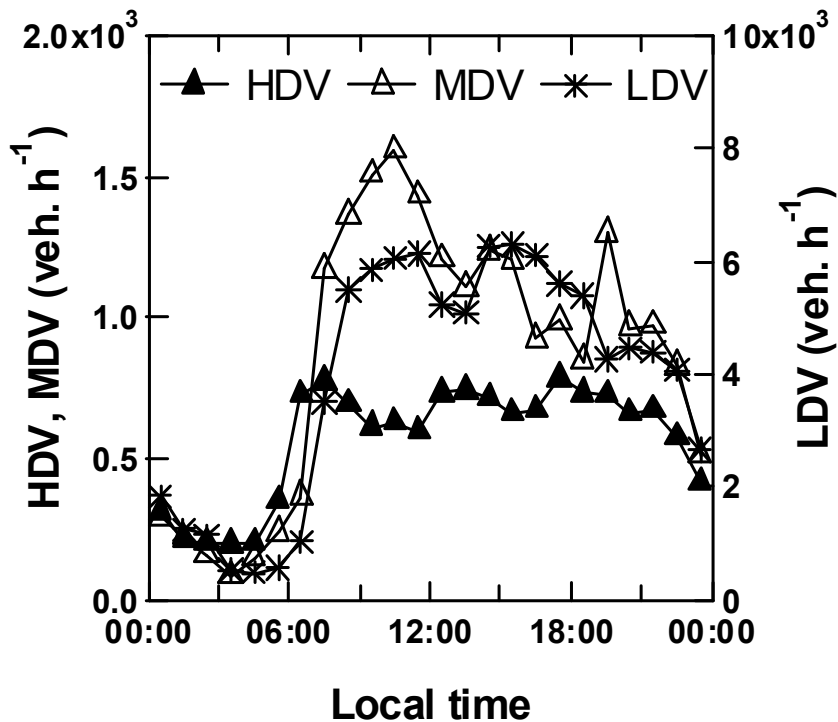


Fig. 2. Diurnal patterns of heavy-duty (HDV), medium-duty (MDV) and light-duty (LDV) vehicles on the Dongfeng middle road, recorded during 18–24 July 1999 and 12–18 October 1999 (Xie et al., 2003).

[Title Page](#)[Abstract](#)[Introduction](#)[Conclusions](#)[References](#)[Tables](#)[Figures](#)[◀](#)[▶](#)[◀](#)[▶](#)[Back](#)[Close](#)[Full Screen / Esc](#)[Printer-friendly Version](#)[Interactive Discussion](#)

Elemental carbon in
Guangzhou

R. L. Verma et al.

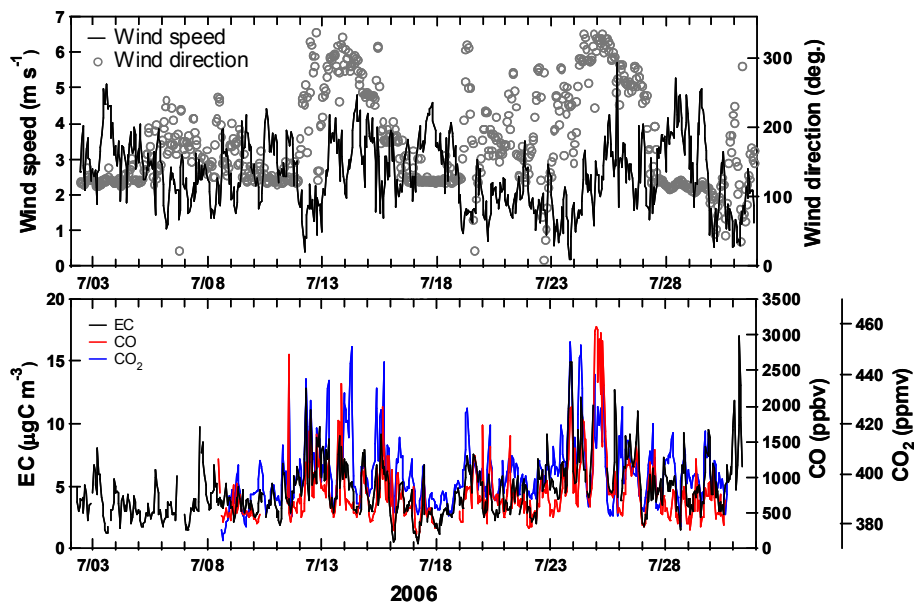


Fig. 3. Time series variations of hourly averaged concentrations of EC, CO, CO₂ and some meteorological parameters.

[Title Page](#)[Abstract](#)[Introduction](#)[Conclusions](#)[References](#)[Tables](#)[Figures](#)[◀](#)[▶](#)[◀](#)[▶](#)[Back](#)[Close](#)[Full Screen / Esc](#)[Printer-friendly Version](#)[Interactive Discussion](#)

Elemental carbon in
Guangzhou

R. L. Verma et al.

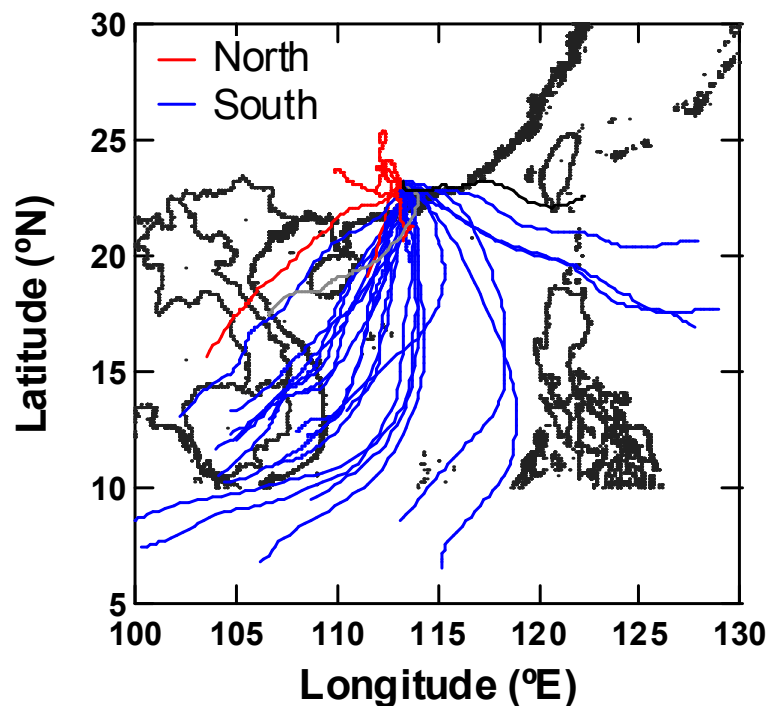


Fig. 4. Three-day back trajectories each started at 00:00 LT from observation site (23.13° N, 113.26° E, and 50 m a.g.l.). The trajectories were calculated using HYSPLIT-4 model (NOAA/ARL, FNL meteorological archived dataset).

[Title Page](#)[Abstract](#)[Introduction](#)[Conclusions](#)[References](#)[Tables](#)[Figures](#)[I◀](#)[▶I](#)[◀](#)[▶](#)[Back](#)[Close](#)[Full Screen / Esc](#)[Printer-friendly Version](#)[Interactive Discussion](#)

Elemental carbon in
Guangzhou

R. L. Verma et al.

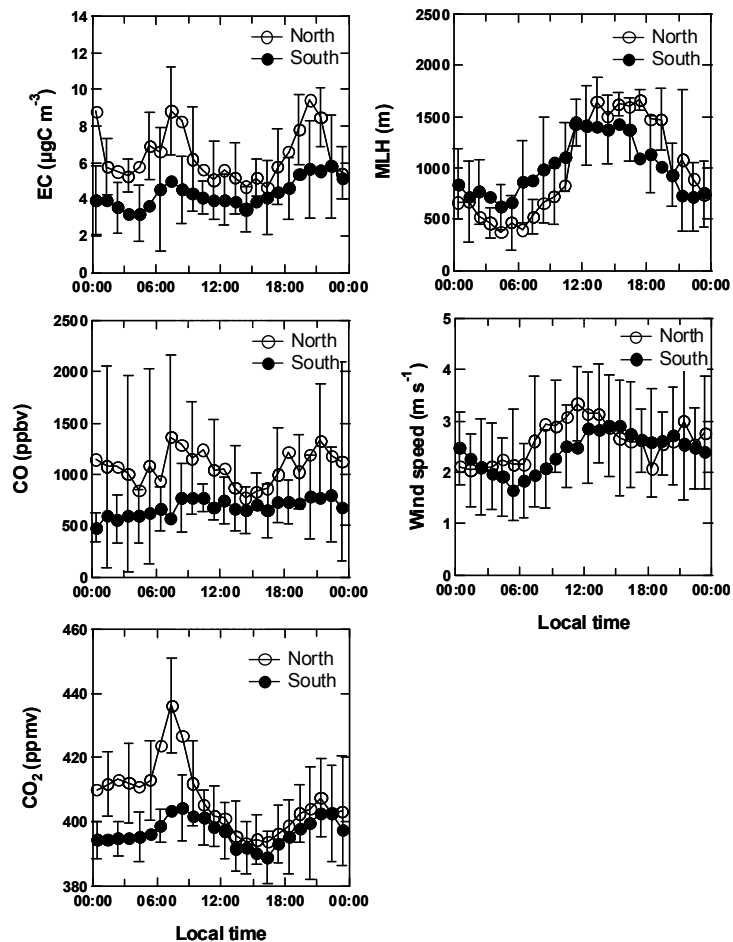


Fig. 5. Diurnal variations of hourly average \pm SD of EC, CO, CO₂, wind speed, and mixed layer height (MLH).

[Title Page](#)[Abstract](#)[Introduction](#)[Conclusions](#)[References](#)[Tables](#)[Figures](#)[I ◀](#)[▶ I](#)[◀](#)[▶](#)[Back](#)[Close](#)[Full Screen / Esc](#)[Printer-friendly Version](#)[Interactive Discussion](#)

Elemental carbon in
Guangzhou

R. L. Verma et al.

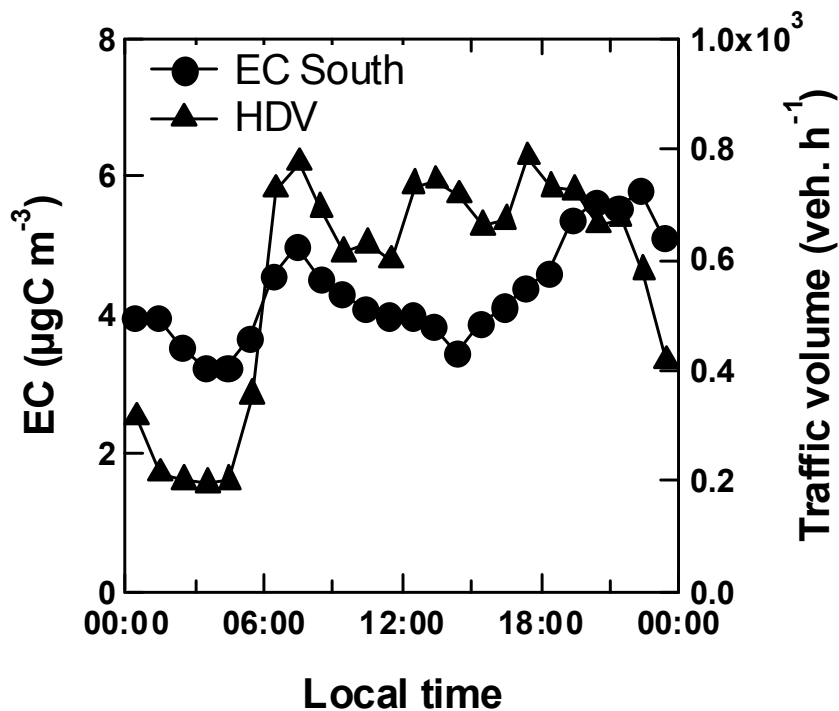


Fig. 6. Diurnal variations of hourly EC and heavy-duty vehicles (HDV) in Guangzhou.

[Title Page](#)[Abstract](#)[Introduction](#)[Conclusions](#)[References](#)[Tables](#)[Figures](#)[I◀](#)[▶I](#)[◀](#)[▶](#)[Back](#)[Close](#)[Full Screen / Esc](#)[Printer-friendly Version](#)[Interactive Discussion](#)

Elemental carbon in
Guangzhou

R. L. Verma et al.

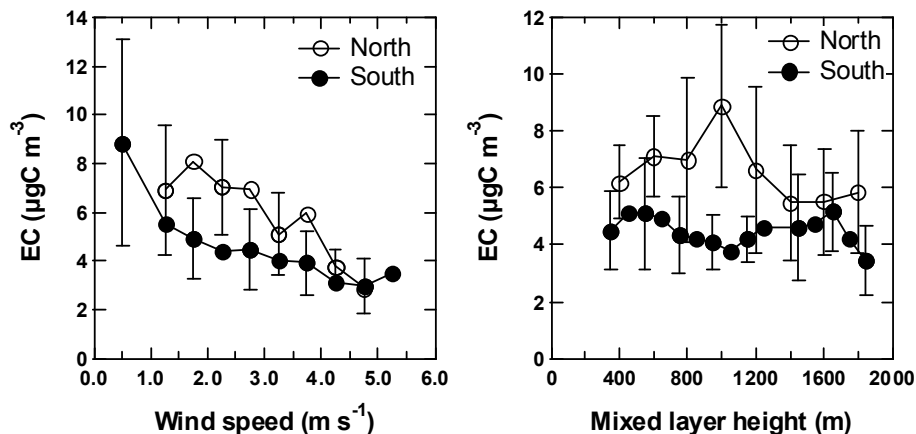


Fig. 7. Dependencies of EC on wind speed and MLH, calculated for each 0.5 ms^{-1} of wind speed and 100 m (200 m for north) bins of MLH, respectively. Data observed between 09:00 to 21:00 LT have been used for the calculation of dependencies of EC.

[Title Page](#)[Abstract](#)[Introduction](#)[Conclusions](#)[References](#)[Tables](#)[Figures](#)[I◀](#)[▶I](#)[◀](#)[▶](#)[Back](#)[Close](#)[Full Screen / Esc](#)[Printer-friendly Version](#)[Interactive Discussion](#)

Elemental carbon in
Guangzhou

R. L. Verma et al.

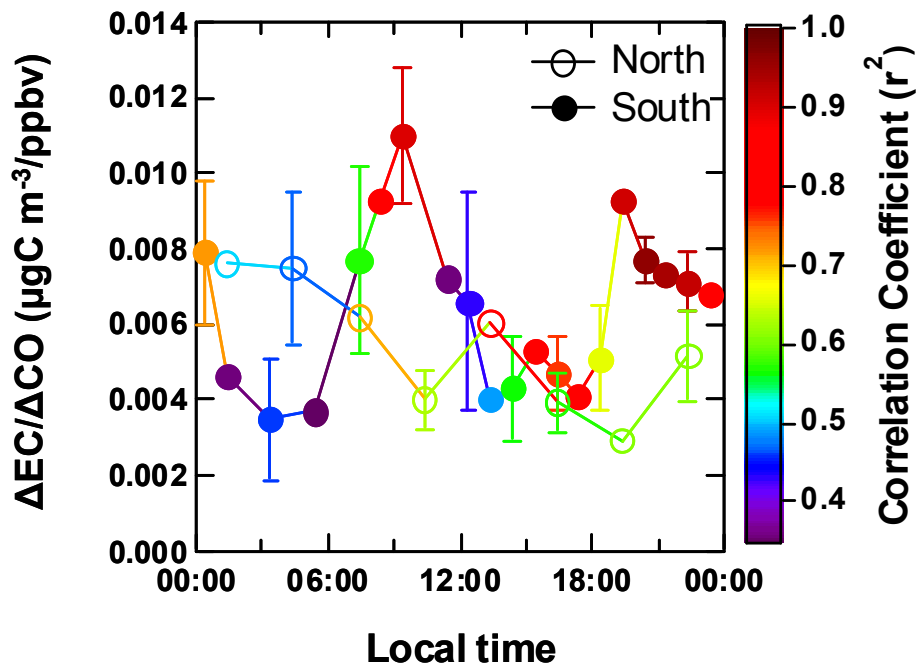


Fig. 8. Diurnal variations of $\Delta EC/\Delta CO$ linear regression slopes (\pm SD bar) (3-h for northern and 1-h for southern air masses) and r^2 . Missing data points are for $r^2 < 0.35$.

[Title Page](#)[Abstract](#)[Introduction](#)[Conclusions](#)[References](#)[Tables](#)[Figures](#)[I◀](#)[▶I](#)[◀](#)[▶](#)[Back](#)[Close](#)[Full Screen / Esc](#)[Printer-friendly Version](#)[Interactive Discussion](#)

Elemental carbon in
Guangzhou

R. L. Verma et al.

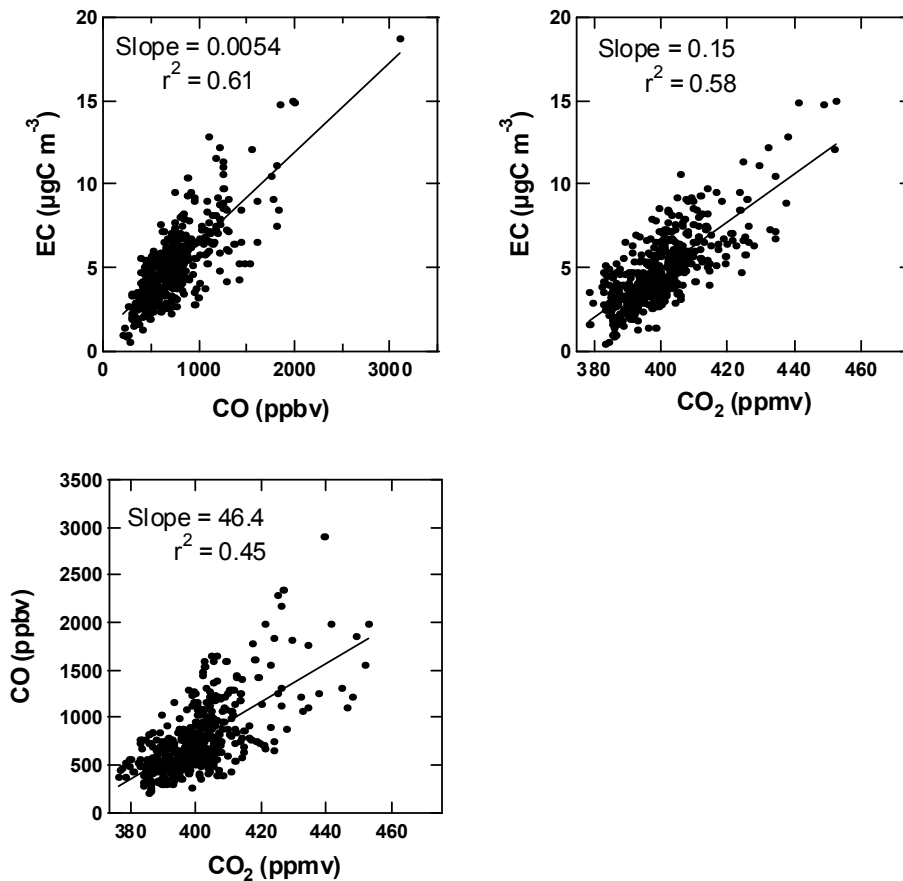


Fig. 9. Scatter plots of EC-CO, EC- CO_2 , and CO- CO_2 measured during the campaign.

[Title Page](#)[Abstract](#)[Introduction](#)[Conclusions](#)[References](#)[Tables](#)[Figures](#)[I◀](#)[▶I](#)[◀](#)[▶](#)[Back](#)[Close](#)[Full Screen / Esc](#)[Printer-friendly Version](#)[Interactive Discussion](#)

Elemental carbon in
Guangzhou

R. L. Verma et al.

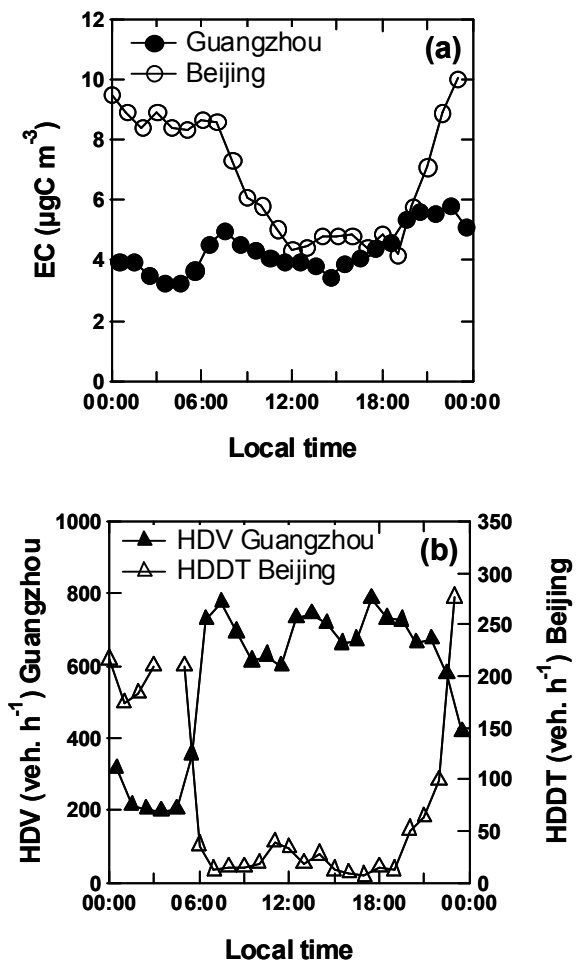


Fig. 10. Diurnal variations of (a) EC and (b) heavy-duty vehicles in Guangzhou and Beijing.

[Title Page](#)[Abstract](#)[Introduction](#)[Conclusions](#)[References](#)[Tables](#)[Figures](#)[I <](#)[> I](#)[◀](#)[▶](#)[Back](#)[Close](#)[Full Screen / Esc](#)[Printer-friendly Version](#)[Interactive Discussion](#)

Elemental carbon in
Guangzhou

R. L. Verma et al.

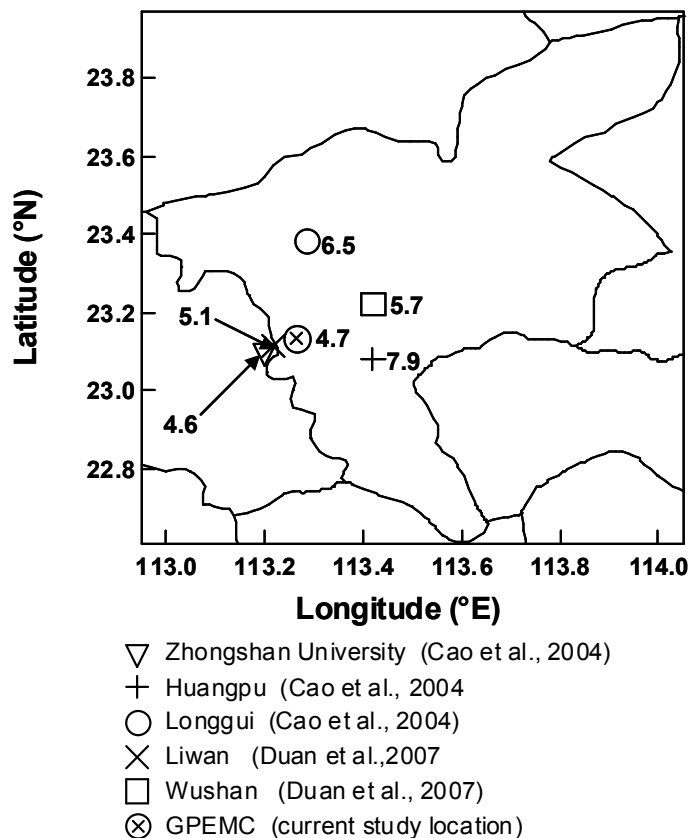


Fig. 11. Sites where EC concentrations (μgCm^{-3}) were measured during present study and previous campaigns in summer season.

[Title Page](#)[Abstract](#)[Introduction](#)[Conclusions](#)[References](#)[Tables](#)[Figures](#)[I◀](#)[▶I](#)[◀](#)[▶](#)[Back](#)[Close](#)[Full Screen / Esc](#)[Printer-friendly Version](#)[Interactive Discussion](#)